Biomaterials

DOI: 10.1002/anie.201200591

Artificial Egg Stalks Made of a Recombinantly Produced Lacewing Silk Protein**

*Felix Bauer and Thomas Scheibel**

For decades, silk has inspired scientists because of its mechanical properties (combined tensile strength, extensibility, and toughness), good biocompatibility, and biodegradability. Silks can be envisioned for several applications, ranging from automotive applications, for example, airbags, to medical devices, such as nerve conduits or drug delivery.[1–8] Lacewings (Figure 1 A) use silk fibers as egg stalks. In contrast to other silks, egg stalk silk has a cross β structure, which was already determined in 1957.[9] Since then, only a few additional cross β silks have been identified.[10] In the species *Chrysopa carnea*, the silk dope contains five abundant proteins (Figure 1 B), and in the species *Mallada signata*, two serine- and glycine-rich proteins (MalXB1 (86 kD) and MalXB2 (55.5 kD)) have been identified. Both MalXB proteins have highly repetitive core domains and small terminal domains.[11] The putative structure of the core domain of both proteins is rich in β sheet, with a predicted sheet length of four amino acids followed by turns (Supporting Information, Figure S1). For the production of egg stalks, the lacewing simply deposits a droplet of silk dope on a surface and dips in an egg. Pulling the egg creates a filament which hardens within a few seconds. In nature, stalks hang downwards from leaves, but if turned around they do not bend under the load of the egg (Figure 2 B). However, at high humidity, lacewing egg stalks show an extensibility of up to 600 %.[11]

To biomimetically produce an egg stalk with similar properties, we engineered and recombinantly produced an artificial egg stalk protein. Owing to the repetitive character of the identified egg stalk proteins, it was possible to generate a consensus motif for the core domain of MalXB2, which we named [AS]. The motif comprises 48 amino acids (Figure 1 D; Supporting Information, Figure S1). Similar to engineering of highly repetitive spider silk proteins,[12,13] we multimerized the DNA encoding this module to mimic the repetitive core sequence using a seamless cloning technique as described previously.[12] Sequences encoding the terminal domains were ligated yielding an engineered gene with a codon usage optimized for expression in *E. coli*. The engineered protein N[AS]$_8$C contains eight repeats of module [AS], both natural termini, and has a molecular weight of 53 kD, which is similar to that of the natural protein MalXB2.[11] Although SDS-

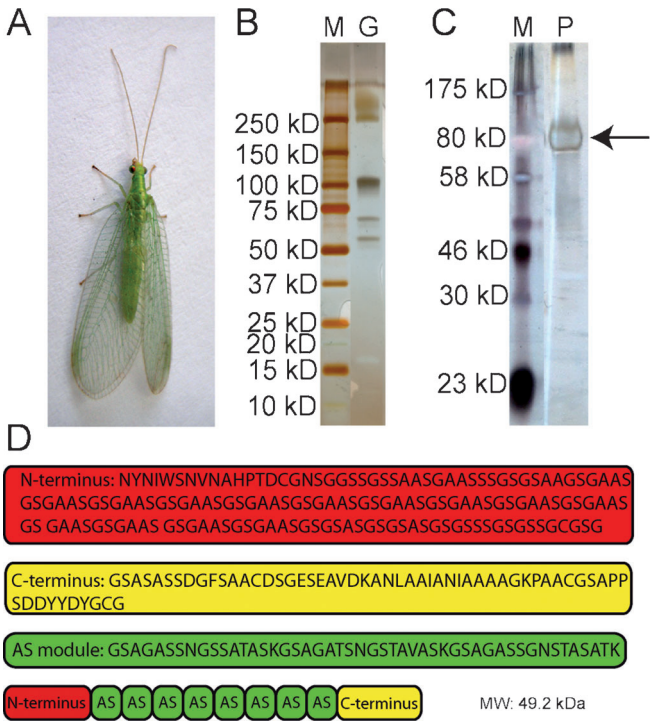

Figure 1. Natural and recombinant lacewing silk. A) Green lacewing *Chrysopa carnea*. B) Dope extracted from a female *Chrysopa carnea* silk gland separated by SDS-PAGE and visualized by silver staining. M = protein marker, G = lacewing silk gland extract. C) Purified recombinant N[AS]$_8$C protein. M = protein marker, P = purified N[AS]$_8$C. D) Designed modules.

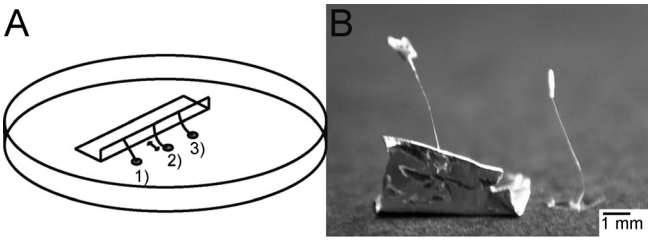

Figure 2. Comparison of natural and artificial stalks. A) Representation of stalk production: 1) stalk drawn from the dope to tinfoil using tweezers; 2) relaxation of the stalk by movement of the tinfoil; 3) stalk contraction during post-treatment at 60 °C and 70 % relative humidity. B) An artificial egg stalk with tinfoil on top (left) and a natural egg stalk with an egg on top (right).

[*] F. Bauer, Prof. Dr. T. Scheibel
Lehrstuhl Biomaterialien, Universität Bayreuth
Universitätsstrasse 30, 95440 Bayreuth (Germany)
E-mail: thomas.scheibel@uni-bayreuth.de
Homepage: http://www.fiberlab.de

[**] The authors thank Christopher Volker Synatschke for assistance with the MALDI-TOF measurements, Johannes Diehl and Claudia Blüm for assistance with the SEM images, and Dr. Andrew Smith, Dr. Martin Humenik, and Lukas Eisoldt for critical appraisal of the manuscript.

Supporting information for this article is available on the WWW under http://dx.doi.org/10.1002/anie.201200591.

PAGE analysis revealed an apparently higher molecular weight for $N[AS]_8C$ than calculated, the correct mass of the protein was confirmed by mass spectrometry (Supporting Information, Figure S2).

Owing to the low solubility of $N[AS]_8C$ in aqueous solutions, we dissolved the protein (10% w/v) in hexafluoroacetone (HFA). In general, HFA induces an α-helical structure in dissolved proteins,[14] and in case of $N[AS]_8C$ this secondary structures was confirmed by circular dichroism (CD) spectroscopy (Supporting Information, Figure S3). Mimicking the silk stalk formation of lacewings, tweezers were dipped in a droplet of $N[AS]_8C$ solution and a fiber was withdrawn. The end of the resulting stalk was transferred to a tinfoil support followed by drying (Figure 2A). For post-treatment, stalks were placed in a climate chamber at 60°C and 70% relative humidity overnight. Other possibilities for post treatment of the stalks would be the use of cosmotropic salt solutions, ethanol, methanol, isopropanol, or high pressure.[15,16]

The artificial stalks have a smooth surface that is similar to natural stalks (Supporting Information, Figure S4). However, necking occurs in natural stalks, which is related to stressing the stalk at high humidity (>30%) or under water. This phenomenon leads to a loss of rigidity in the necked parts accompanied by a transition from a cross-β-sheet to a parallel-β-sheet structure.[9] Such necking was not observed for artificial stalks.

Accordingly, both artificial and natural stalks were structurally analyzed using FTIR spectroscopy (Figure 3). For secondary structure analysis, Fourier self-deconvolution

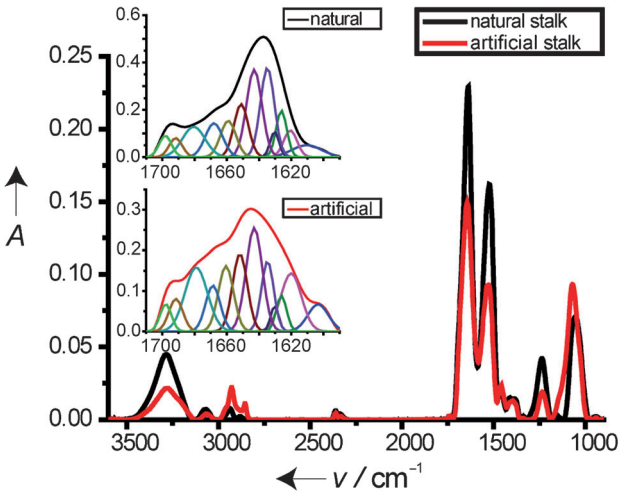

Figure 3. FTIR absorbance spectra of natural and artificial stalks before tensile testing. Insets show the Fourier self-deconvoluted amide I region of natural and artificial stalks.

of the amide I region[17] was performed indicating a lower β-sheet content in artificial stalks in comparison to natural stalks (Table 1). Measuring FTIR spectra before and after stretching of natural and artificial stalks revealed no changes for natural stalks and a slight increase in β-sheet content with a reduced turn content for stretched artificial stalks. The α-helical content in both stalks is quite low at 6–9%. Strikingly,

Table 1: Calculated secondary structure of natural and artificial egg stalks measured before (btt) and after (att) individual tensile testing using FTIR spectroscopy and Fourier self-deconvolution of the amide I band.[17]

Secondary structure	Natural egg stalk		Artificial egg stalk	
	btt [%]	att [%]	btt [%]	att [%]
β sheets	40±6	39±5	32±3	39±4
α helices	6±4	7±1	9±2	7±1
turns	24±3	22±1	30±3	24±1
random coils	30±4	32±2	29±1	30±2

the helical content was also similar before and after stretching. The poly (L-alanine) NCα stretching vibration[18] of natural egg stalks at 1167 cm^{-1}, as detected by polarized FTIR spectra measured at 0° and 90° of the stalk axis, indicates a strong orientation of poly(Ala) β sheets perpendicular to the stalk axis (molecular order parameter: $S^{mol} = -0.44$;[25] Supporting Information, Figure S5). The engineered protein does not contain poly(alanine) sequences, and therefore no orientation could be observed. This indicates that as yet undetected poly(alanine)-rich proteins, probably amongst the three additional proteins detected in *C. carnea* (Figure 1B), could be critically involved in protein alignment in natural stalks. Therefore, our present approach is not suited to fully mimic the natural egg stalk properties.

Both the natural as well as the artificial stalks show birefringence (Figure 4) that is based on structural anisotropy. The birefringence has a high intensity in natural stalks based

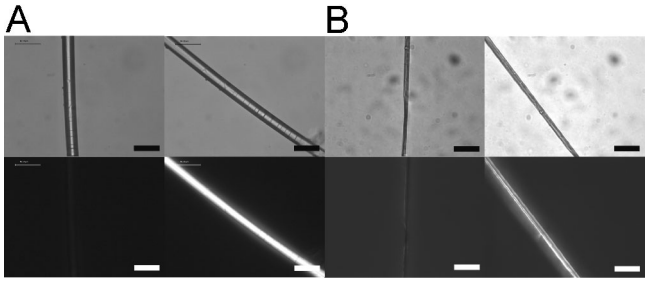

Figure 4. Comparison of birefringence of natural and artificial stalks. A) Microscope images of a natural lacewing egg stalk. B) Microscope images of an artificial egg stalk. Top: bright field; bottom: with crossed polarizers. Scale bars: 50 μm.

on highly ordered crystalline regions with β sheets ordered perpendicular to the stalk axis, while the artificial stalks show weaker birefringence, indicating less but still ordered structures in the stalks.

The artificial stalks have similar diameters (10 μm) as the natural stalks and they reveal a similar apparent rigidity (Figure 2B). Mechanical properties were analyzed at a relative humidity (RH) of 30% and 70% at 22°C. Controlled humidity is highly important for tensile testing of silk.[19–21] The strength of the natural egg stalks (*C. carnea*) is quite low with values of 68 MPa (30% RH) and 155 MPa (70% RH) measured under the chosen conditions, if compared to the published values of 186–375 MPa measured at 65% RH (*Mallada signata* and *Chrysopa spec.*;[11,22] Table 2). At 30%

Table 2: Tensile testing of natural (*C. carnea*) and artificial egg stalks.[a]

	Extensibility [%]	Strength σ_{max} [MPa]	Young's modulus [MPa]	Toughness [MJ m^{-3}]
literature values:[b]				
65% RH[11]	381	310		
65% RH[22]	249	ca. 375		
natural egg stalk:				
30% RH	2±1	68±19	5777±1257	1.2±0.72
70% RH	210±100	155±75	3175±1016	87±49
artificial egg stalk:				
30% RH	5±2	55±14	2330±850	1.76±0.9
70% RH	6±3	25±11	1012±252	1.09±0.59

[a] Experiments were carried out at 30% and 70% relative humidity at 22°C. [b] For *M. signata* and *C. spec.*

RH, the stalks rupture at a strain of about 2%, while at 70% RH they rupture at a strain of 211% (Figure 5 and Table 2). The Young's modulus of natural egg stalks at 30% RH is 5.7 GPa, while the artificial egg stalks have about 40% of the stiffness (2.3 GPa). The tensile strength of the natural stalks is 68 MPa and that of the artificial stalks is 55 MPa (Table 2). Thus, taking the porosity of the artificial stalks into account, a tensile strength of about 63 MPa was calculated (30% RH). Interestingly, the toughness of the artificial stalks at 30% RH is 1.76 MJ m^{-3} and is slightly higher than that of the natural stalks (1.2 MJ m^{-3}).

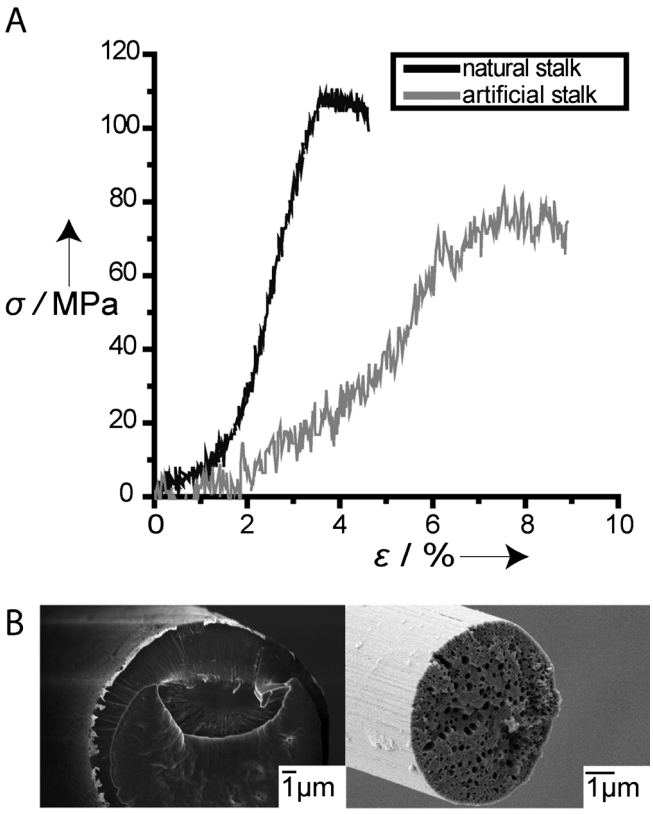

Figure 5. A) Stress–strain curves of the best-performing natural and artificial stalks measured at 30% relative humidity. Differences in noise level are due to smaller stalk diameters in the case of artificial stalks. B) SEM images of cross-sections of a natural stalk (left) and an artificial stalk (right).

The designed and recombinantly produced lacewing egg stalk protein could be processed into artificial stalks with similar properties in relation to natural stalks at 30% RH. The stalks show bending properties that are very similar to the natural stalks, which may open applications for protein fibers, where rigidity in the transversal direction is of interest. Furthermore, the recombinant approach allows the molecular structure–function relationship in egg stalk proteins to be better understood. It will therefore be of importance to identify poly(alanine)-containing eggstalk proteins and to obtain aqueous spinning dopes, which will be necessary to obtain initial structure formation. A pre-structured dope solution will be the key to obtain fibers with cross β structures.

Experimental Section

All of the gene modules (N, [AS], and C) were designed with a 5′-*Bam*HI and a 3′-*Hin*dIII restriction site and obtained from Geneart. Modules were cloned using the enzymes *Bsa*I, *Bsg*I, and *Bse*RI followed by ligation.[12] The complete N[AS]$_8$C construct was transferred to a pET28 vector using *Bam*HI and *Hin*dIII.

BL21 (DE3) cells were transformed with pET28 N[AS]$_8$C and grown in a fermenter (Infors Minifors 2.5 L) using a procedure described previously.[23] At an OD_{600} of 72, the bacteria were induced with 1 mM isopropyl β-D-thiogalactopyranoside (IPTG) for 3 h. Cells were harvested and washed three times.

Purification was performed following a procedure described for other recombinant silk proteins.[24] After cell lysis, acidification, and centrifugation, the supernatant was fractionally precipitated using ammonium sulfate (1.5 M and 2.5 M). The precipitated protein was washed with water and lyophilized.

To analyze the produced protein, N[AS]$_8$C (3 mg mL^{-1}) was dissolved in 6 M guanidinium thiocyanate and diluted to a final concentration of 2 M guanidinium thiocyanate. Before spotting, samples were desalted by ZipTip C4 pipette tips and eluted by matrix solution. MALDI-TOF mass spectrometry was performed on a Bruker Reflex III equipped with a 337 nm N_2 laser in the linear mode and a 20 kV acceleration voltage. Sinapinic acid (20 mg mL^{-1}) was used as the matrix in 50% CH_3CN and 0.1% trifluoroacetic acid in H_2O.

The stalks were pulled out of a droplet of N[AS]$_8$C (10% w/v) in HFA and dried at room temperature. Afterwards, tension was removed from the stalk by moving the contact points closer, and the samples were placed overnight in a climate chamber at 60°C and 70% RH.

For scanning electron microscopy, samples were sputter-coated with platinum (thickness 2 nm). SEM images were obtained with a Zeiss 1530 using the inlens detector.

FTIR spectroscopy was performed using a Bruker tensor 27/pike MIRacle using a Hyperion unit. Data processing and Fourier self-deconvolution of the amide I region was performed using the Opus 6.5 software.[17] Polarized FTIR measurements and processing of the data was done according to Hagenau et al.[25]

Microscope images were obtained using a Leica DMI 3000B microscope equipped with polarizers.

Samples for tensile testing were glued with plastic glue onto plastic frames having a gauge length of 2 mm. Stress–strain curves

were recorded on a tensile tester (Bose Electroforce 3220) equipped with a 0.5 N load cell using a climate chamber to adjust the relative humidity. The stalks were extended with a rate of 0.01 mm s^{-1} until they ruptured.

Circular dichroism spectra were recorded from 250 nm to 195 nm using a Jasco J-815 CD spectrometer measuring with an interval of 0.1 nm, a bandwidth of 1 nm, a scanning speed of 50 nm min^{-1}, a digital integration time (D.I.T.) of 1 s, and three accumulations.

Received: January 20, 2012
Revised: April 10, 2012
Published online: May 16, 2012

Keywords: β sheets · biomimetic systems · fiber proteins · lacewing · silk

[1] J. G. Hardy, T. R. Scheibel, *Prog. Polym. Sci.* **2010**, *35*, 1093 – 1115.
[2] A. Leal-Egana, T. Scheibel, *Biotechnol. Appl. Biochem.* **2010**, *55*, 155 – 167.
[3] A. Lammel, M. Schwab, M. Hofer, G. Winter, T. Scheibel, *Biomaterials* **2011**, *32*, 2233 – 2240.
[4] C. Allmeling, A. Jokuszies, K. Reimers, S. Kall, C. Y. Choi, G. Brandes, C. Kasper, T. Scheper, M. Guggenheim, P. M. Vogt, *Cell Proliferation* **2008**, *41*, 408 – 420.
[5] C. Allmeling, A. Jokuszies, K. Reimers, S. Kall, P. M. Vogt, *J. Cell. Mol. Med.* **2006**, *10*, 770 – 777.
[6] K. Spiess, A. Lammel, T. Scheibel, *Macromol. Biosci.* **2010**, *10*, 998 – 1007.
[7] S. Weisman, V. S. Haritos, J. S. Church, M. G. Huson, S. T. Mudie, A. J. Rodgers, G. J. Dumsday, T. D. Sutherland, *Biomaterials* **2010**, *31*, 2695 – 2700.
[8] J. G. Hardy, L. M. Romer, T. R. Scheibel, *Polymer* **2008**, *49*, 4309 – 4327.
[9] K. D. Parker, K. M. Rudall, *Nature* **1957**, *179*, 905 – 906.
[10] C. L. Craig, *Annu. Rev. Entomol.* **1997**, *42*, 231 – 267.
[11] S. Weisman, S. Okada, S. T. Mudie, M. G. Huson, H. E. Trueman, A. Sriskantha, V. S. Haritos, T. D. Sutherland, *J. Struct. Biol.* **2009**, *168*, 467 – 475.
[12] D. Huemmerich, C. W. Helsen, S. Quedzuweit, J. Oschmann, R. Rudolph, T. Scheibel, *Biochemistry* **2004**, *43*, 13604 – 13612.
[13] C. Vendrely, T. Scheibel, *Macromol. Biosci.* **2007**, *7*, 401 – 409.
[14] J. M. Yao, H. Masuda, C. H. Zhao, T. Asakura, *Macromolecules* **2002**, *35*, 6 – 9.
[15] H. Peng, S. Zhou, J. Jiang, T. Guo, X. Zheng, X. Yu, *J. Phys. Chem. B* **2009**, *113*, 4636 – 4641.
[16] X. Zhang, M. R. Reagan, D. L. Kaplan, *Adv. Drug Delivery Rev.* **2009**, *61*, 988 – 1006.
[17] X. Hu, D. Kaplan, P. Cebe, *Macromolecules* **2006**, *39*, 6161 – 6170.
[18] W. H. Moore, S. Krimm, *Biopolymers* **1976**, *15*, 2465 – 2483.
[19] A. Schäfer, T. Vehoff, A. Glisovic, T. Salditt, *Eur. Biophys. J. Biophys. Lett.* **2008**, *37*, 197 – 204.
[20] T. Vehoff, A. Glisovic, H. Schollmeyer, A. Zippelius, T. Salditt, *Biophys. J.* **2007**, *93*, 4425 – 4432.
[21] G. R. Plaza, G. V. Guinea, J. Perez-Rigueiro, M. Elices, *J. Polym. Sci. Part B* **2006**, *44*, 994 – 999.
[22] H. R. Hepburn, H. D. Chandler, M. R. Davidoff, *Insect Biochem.* **1979**, *9*, 69 – 77.
[23] D. J. Korz, U. Rinas, K. Hellmuth, E. A. Sanders, W. D. Deckwer, *J. Biotechnol.* **1995**, *39*, 59 – 65.
[24] X.-X. Xia, Z.-G. Qian, C. S. Ki, Y. H. Park, D. L. Kaplan, S. Y. Lee, *Proc. Natl. Acad. Sci. USA* **2010**, *107*, 14059 – 14063.
[25] A. Hagenau, P. Papadopoulos, F. Kremer, T. Scheibel, *J. Struct. Biol.* **2011**, *175*, 339 – 347.

